ZRO$_2$ AND UO$_2$ DISSOLUTION BY MOLTEN ZIRCALLOY

J. Stuckert, A. Miassoedov, P. J. Hayward, P. Hofmann, M. Veshchunov
Forschungszentrum Karlsruhe
Hermann-von-Helmholtz –Platz 1, D-76344 Eggenstein-Leopoldshafen
juri.stuckert@imf.fzk.de, alexei.miassoedov@imf.fzk.de

ABSTRACT

This paper describes the results of the different tests on the dissolution of ZrO$_2$ and UO$_2$ by molten Zircaloy at temperatures about 1000 K below their melting point. The understanding of the mechanisms of this process is important for the modelling of the fuel rod failure during the reactor severe accidents.

1   INTRODUCTION

The fuel material dissolution by Zry-rich melts occurs in the core during the progression of a severe accident. It has profound consequences on the course of the accident in nuclear reactors in which severe damage to the core occurs. It can be responsible for large amounts of fuel liquefaction at temperatures well below the UO$_2$ melting point ($\approx$2850 °C), it can affect the corium composition and the timing of H$_2$ production and fission products release. Finally it is responsible for the loss of the original core geometry.

Just after the Zry melting, which occurs between 1760 to 1980 °C depending on its oxygen content, the fuel dissolution by molten Zry starts. This interaction is the main cause of the UO$_2$ liquefaction and is very rapid above 2250 °C. Large amounts of U-Zr-O mixtures can be produced with up to 80 wt% of dissolved UO$_2$ [1]. In the reactor case, the UO$_2$ dissolution by molten Zry occurs simultaneously with the dissolution of the external ZrO$_2$ layer of the fuel rod cladding.

At the end of the early phase (700 °C – 2200 °C) of the core degradation just after the Zry melting, the metallic Zry trapped between the UO$_2$ pellets and the external ZrO$_2$ layer on the cladding (in the rod geometry) will induce a simultaneous dissolution of UO$_2$ and ZrO$_2$. Once the U-Zr-O melt has formed, the external ZrO$_2$ shell can fail. The clad failure criteria due to chemical interactions is not well known up to now. Usually it is expected to depend on the thickness of the ZrO$_2$ shell and on the fuel rod temperature. After the cladding failure, the U-O-Zr melt flows downwards to the lower core region. The loss of rod-like geometry corresponds to the onset of the late phase of core degradation. Major part of the core inventory of gaseous and volatile fission products is released at this time.

The ceramic dissolution phenomena are important also for the late phase of the core degradation scenario. Namely by the formation of the molten pool: as the process of solidification of relocating metallic melt with dissolved UO$_2$ and ZrO$_2$ continues, a crust will form local blockages and acts as a crucible for melt which arrives later.

2   DISSOLUTION OF FRESH UO$_2$ BY MOLTEN ZRY

Crucible tests were carried out by AECL (Canada) and FZK (Germany) [2]. The intention was to reconcile the differences in previously published data for fuel dissolution by the molten cladding, in particular regarding the limit of the dissolution for which previous AECL tests showed a limitation at the end of the precipitation stage. This was not observed in the previous FZK tests.

Typical test results of UO$_2$ crucibles after interaction with molten Zircaloy with and without Y$_2$0$_3$ disc placed at the bottom of the crucible cavity are shown in Figures 1 and 2. Attack and dissolution of the UO$_2$ crucible by the molten Zircaloy can be clearly recognised.

The post-test examinations showed that all solidified melts contained the same three phase types in variable amounts:

- α-Zr(O) alloy phase, which formed the matrix,
- ceramic (U,Zr)O $_{2-x}$ phase,
- metallic U(O) phase containing minor amounts of Zr and Sn.

These various phases are shown in Figures 3 and 4. Similar phases and microstructures occurred uniformly throughout the solidified melts.
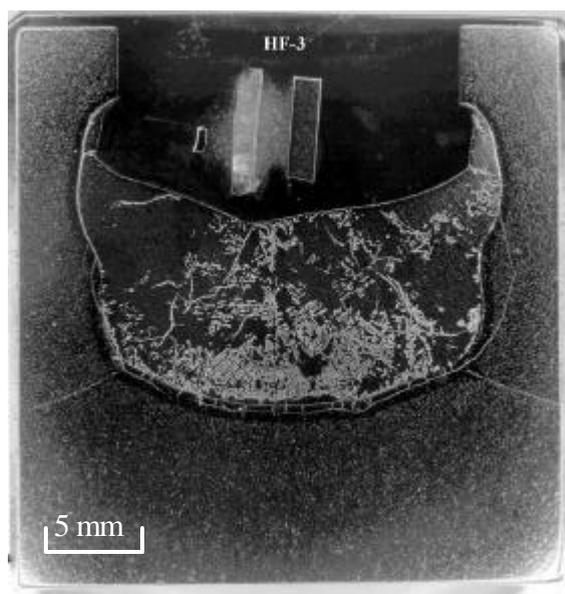
Figure 1: Cross section of UO$_2$ crucible, as-polished, 2100 °C. Crucible geometric density 10.5 g/cm³
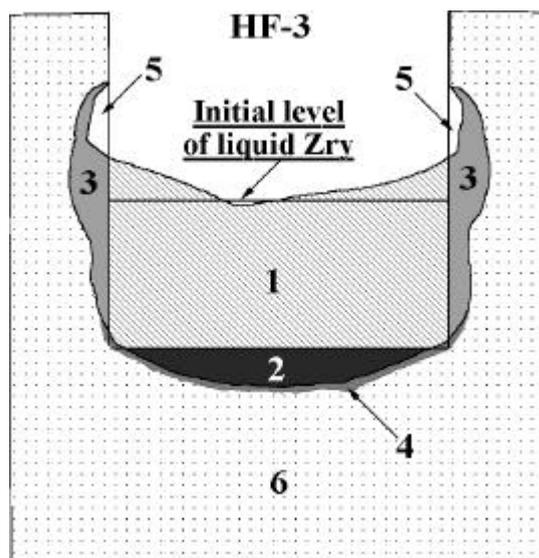
Figure 2: Typical interaction zones in UO$_2$ crucible: 1 – initial Zry-melt, 2,3,5 – dissolved parts of crucible 6 – initial crucible
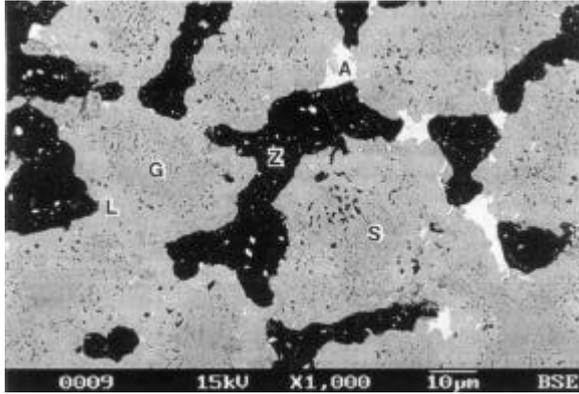
Figure 3: BSE micrograph of the central melt region in the HF-15 specimen (2200°C, 428 s). G = Zr-rich inner ceramic zone; L = outer ceramic zone; Z = Zr(O) alloy; A = U(O) alloy; S = inclusions of Zr(O) in the ceramic phase
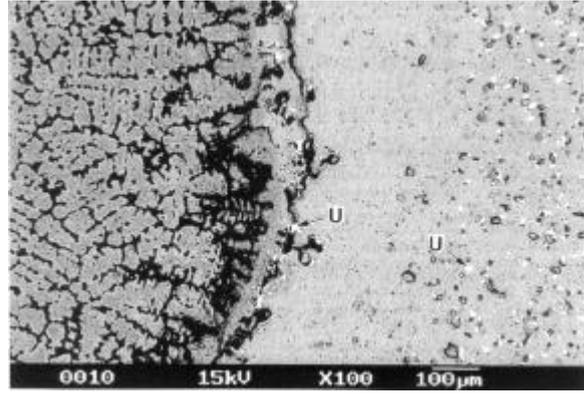
Figure 4: BSE micrograph of the right melt/crucible interface in the HF-26 specimen (2200°C, 853 s), showing U metal precipitates (U) at the interface and in the residual crucible, separated by a ~300-μm U-free zone

3   UO₂ DISSOLUTION MODELLING

Recently it was demonstrated [3] that in the crucible tests the bulk melt composition attains its saturation value during the short time interval of the first *saturation period*. The time duration of this saturation phase depends on the ratio of *S/V* (interaction surface to melt volume). In the subsequent time interval *(precipitation period)* the continued oxygen supply to the interface by *diffusion* from fuel interior leads to an oversaturation of the melt, resulting in precipitation of the ceramic $(U,Zr)O_{2-x}$ phase in the melt. Simultaneously, slow dissolution of solid UO_2 can be continued. The kinetic of the process during this stage depends from the oxygen content in the crucible wall, i.e. from the thickness of ceramic wall.

Figure 5 shows the experimental (Inductively Coupled Plasma analysis) and calculation results of the uranium content in the melt.
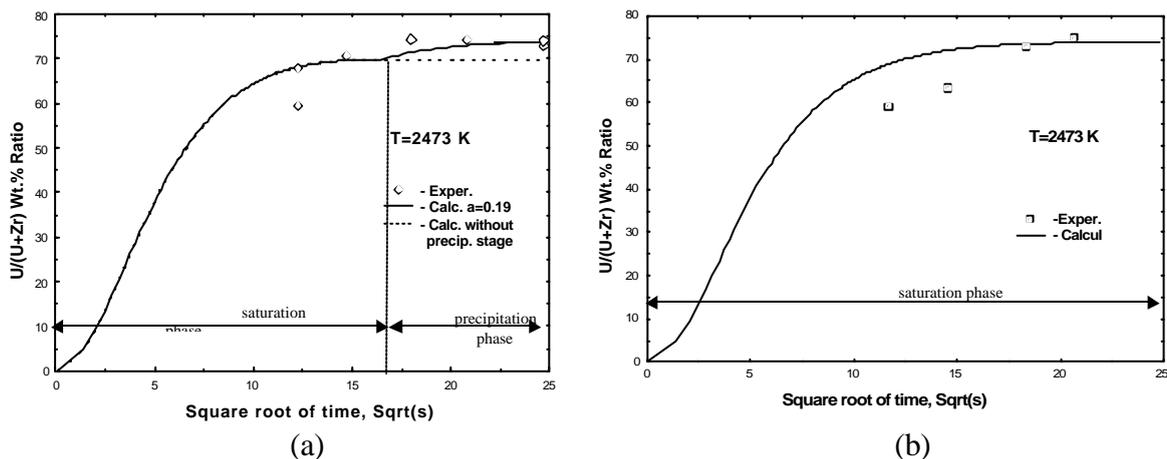

(a)   (b)

Figure 5: Simulations of the AECL/FZK crucible tests on UO₂ dissolution by molten Zry. Time evolution of uranium weight content in the melt at T=2200 °C in the tests without (a) and with (b) bottom isolation. Parameter α denotes composition of the ceramic $(U_{1-\alpha}Zr_\alpha)O_{2-x}$ precipitates

4   DISSOLUTION OF IRRADIATED UO$_2$ BY MOLTEN ZRY

Due to the modification of the UO$_2$ morphology induced by the irradiation effects, the burn-up affects the core degradation, in particular the fuel dissolution kinetics and the related fission products release. Different separate-effects tests were carried out by JRC-ITU (Karlsruhe) [4] in order to evaluate the burn-up impact on the UO$_2$ dissolution by molten Zr. The samples (segments of cladded irradiated fuel) were of high enrichment fuel (8.3% U-235) and had a burn-up of 53 GWd/tU.

The porosity in the irradiated fuel at 2000 °C is considerable and reaches 30%, in contrast to the non-irradiated fuel, due to the fission gases and volatiles collected in bubbles and grain boundary pores. This will cause an acceleration of the irradiated fuel dissolution with time compared to the uniform fuel dissolution of non-irradiated fuel. The tests at 2000 °C with irradiated and non-irradiated fuel show substantial differences with a more rapid dissolution of the irradiated fuel. This can be attributed to the additional cracks and irregularities of the irradiated material (the non-irradiated fuel breaks up into larger, more geometric pieces). Though the sample geometries were different, the comparison implied a considerably faster dissolution of the irradiated fuel at 2000 °C with a rate similar to the expected one obtained by the interpolation for the non-irradiated fuel at 2150 °C.

The indication of an effective difference in dissolution rates between irradiated and non-irradiated fuel of about 150 °C at 2000 °C could nevertheless be useful for a provisional model in severe accident codes to take into account the burn-up effect on the UO$_2$-Zry dissolution.

5   ZRO$_2$ DISSOLUTION BY MOLTEN ZIRCALOY

During a high-temperature transient in a severe accident, the outer surfaces of Zry cladding will be oxidised, forming a layer of ZrO$_2$. After reaching the melting point of the underlying non-oxidised Zry layer, the molten Zr(O) alloy, held in contact with the fuel by the outer ZrO$_2$ layer, will begin to dissolve both UO$_2$ fuel and ZrO$_2$ simultaneously until failure of the oxide layer occurs. Thus, the dissolution of the outer ZrO$_2$ layer of the cladding and its failure are important factors for determining:
   - the residence time of UO$_2$ dissolution by molten Zry, and
   - the amount and O$_2$ content of the molten α-Zr(O) which drive the UO$_2$ dissolution.

Isothermal heating experiments within the temperature range from 2100 °C to 2300 °C and with annealing times of up to 300 min in argon atmosphere have been performed by FZK to study the dissolution of zirconia crucibles by molten Zircaloy [5]. The tests were performed with large CaO-stabilized zirconia crucibles (geometric density 5.3 g/cm³, ratio S/V=350 m^{-1}) and with small Y$_2$O$_3$-stabilised zirconia crucibles (geometric density 5.8 g/cm³, ratio S/V=700 m^{-1}). In the crucibles oxygen-free Zry-4 charges were installed.

The post-test examinations showed a white metallic-looking stripe around the circumference on the outer surface of some crucibles. The height of the stripes corresponds to the height of the melt. This stripe was identified by SEM/EDX analysis as metallic α-Zr(O) precipitates within the ZrO$_2$ crucible matrix. Microscope examinations of the sectionned specimens showed the formation of α-Zr(O) precipitates along the grain boundaries in the crucible wall matrix. These investigations show, that the oxygen diffuses to the melt mainly from the surface of the ceramic grains.

The image analysis of the melt microstructure allows to determine the content of the ceramic part in the melt and to calculate the oxygen content in the melt. These calculation results show, that almost in all experiments with the small crucibles the melt composition at the temperature corresponds to the two-phase area on the Zr-O phase diagram (ceramic

precipitates in the liquid). Therefore for the ZrO_2 dissolution analogous to the UO_2 dissolution one can indicate two typical phases of the process: saturation and precipitation phases. But for the ZrO_2 dissolution formation of the transition layer at the crucible/melt interface is typical (Figure 6). The formation and the growth of a ZrO_{2-x} transition layer at the crucible/melt interface was observed in the tests with small crucibles (completion of the wall dissolution was reached) and not observed for the large crucibles (completion of the wall dissolution was not reached). Because of the transition layer formation two typical phases during the interaction between the melt and ZrO_2 ceramic were named *erosion* (wall dissolution) stage and *corrosion* (transition layer formation) stage.
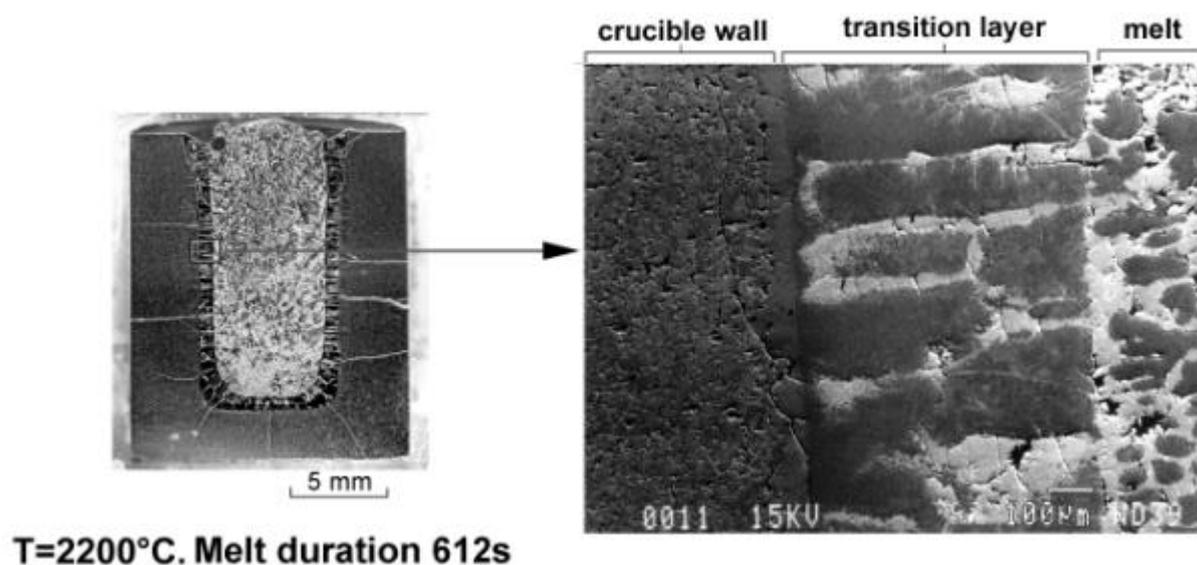

Figure 6: Formation of the ZrO_{2-x} transition layer at the crucible/melt interface

The mass of the dissolved part of the crucible was calculated by means of the image analysis of longitudinal crucible cross-section. This procedure allowed to determine the amount of oxygen transported to the melt from the dissolved part of the crucible. The image and chemical analysis have shown that less oxygen was transported to the melt from the dissolved part of the crucible, than diffused from the undissolved crucible part.

6   COMPARISON OF THE SEPARATE UO₂ AND ZRO₂ DISSOLUTION PROCESSES

The image analysis method to determine the dissolved crucible wall volume and the oxygen concentration was applied for analysis of the tests performed with UO_2 and ZrO_2 crucibles. The comparison of the dissolution rates for UO_2 and ZrO_2, shows that under the same conditions (geometry and temperature) the dissolution process is more rapid for UO_2 than for ZrO_2.

7   ZRO₂ DISSOLUTION MODELLING

The Zr/ZrO_2 dissolution model is based on the balances of oxygen and zirconium masses and interface fluxes. The model includes kinetic parameters such as k_O (mass transfer coefficient in the melt), $D_O^{(ZrO2)}$ (oxygen diffusion coefficient in the oxide), $C_O(I)$ (equilibrium solid/melt interface oxygen concentration in the melt). Comparison of the model against these test data is presented in Figure 7. The main discrepancies occur at the late stage of corrosion which might be associated with formation of ceramic ZrO_2 precipitates in the melt bulk which is not considered in the present model.
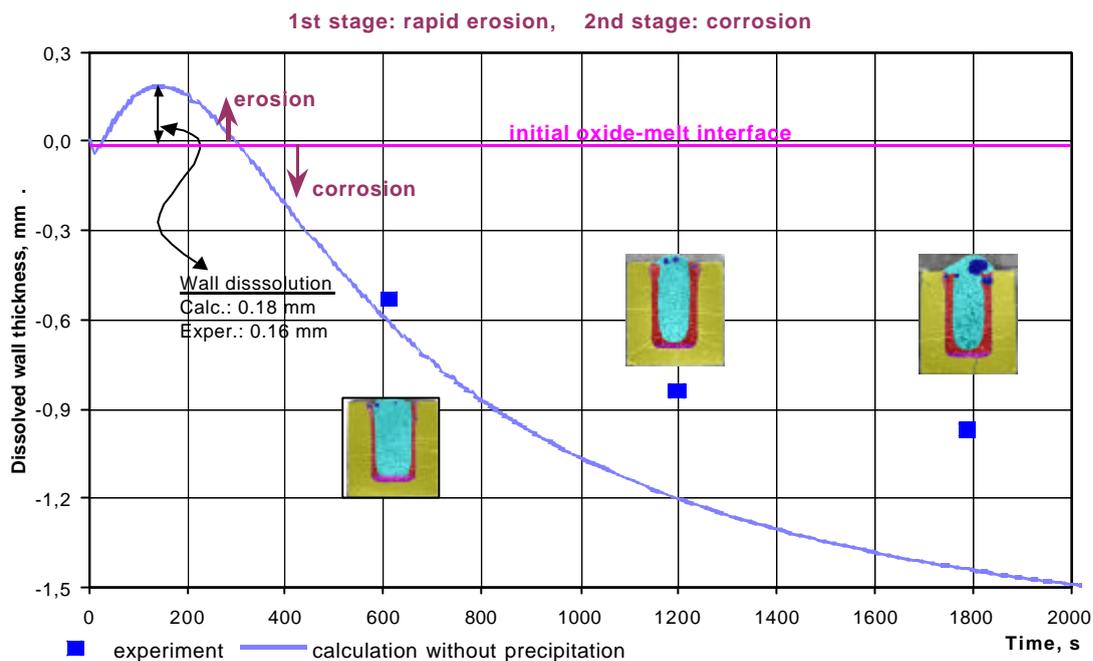
Figure 7: Validation of the ZrO_2 dissolution model against test data on ZrO_2 crucible wall dissolution by molten Zry at 2200 °C

8   FZK CLAD FAILURE TESTS

The dissolution of ZrO_2 by molten Zry is a possible cause of the clad failure, therefore an additional objective of the experimental programme is aimed at determining the clad failure conditions in the rod geometry. If a sufficiently thick oxide layer has formed on the outer surface of the cladding tube, the relocation of molten Zircaloy will be prevented, or limited inside the gap between the cladding and the fuel pellets, because of a "crucible effect" due to the high melting point of ZrO_2. The external oxide layer of the cladding will remain in place until its melting point is reached, or until it is dissolved by molten Zircaloy, or until it fails mechanically. The knowledge of cladding failure mechanisms above the Zircaloy melting temperature is currently lacking. Only simple parametric models using user-defined parameters are currently available in the severe accident code systems. In the assumption currently made, the ZrO_2 layer fails when a certain temperature limit is exceeded (typically in the 2000-2200 °C temperature range) and the ZrO_2 layer is less than a limiting thickness. In some models, the oxide shell is assumed not to break if typically more than 60 % of the cladding has been completely oxidised.

Different experimental approaches have been applied to obtain the required data, however, only the experiments in the small-scale FZK QUENCH test apparatus have been successful. The tube specimen of a length of 50 mm, filled with ZrO_2 pellets, was suspended inside a quartz tube which is surrounded by an induction heating coil. The heat-up rate was varied from 2 K/s to 10 K/s. The ZrO_2 rods were inductively heated up to 1400 °C in (Ar+O_2) mixture to pre-oxidise them (4.5 min to 9 min) to a pre-determined ZrO_2 layer thickness and were then quickly heated up with a rate of 4 K/s or 8 K/s until cladding failure and release of the molten material occurred. The cladding surface temperature was measured by a pyrometer in the centre of the specimen in all tests. In some tests, a centreline thermocouple was used additionally.

The results of the experiments show a clear correlation between the heat-up rate and the oxide shell failure temperature:

- no failure occurs if a heat-up rate is less than 3 K/s: the cladding completely oxidises before reaching the melting point of the Zircaloy;
- for heat-up rates greater than 3 K/s, the cladding failure temperature continuously decreases with increasing heat-up rate and after reaching a certain limit (in our case ~ 6 K/s) remains constant.

After the tests the tube specimen was cut at the location where cladding failure occurred and metallographically prepared to determine the thickness of the remaining ZrO_2 layer. It was detected, that the oxide layer thickness at onset of failure decreases with increasing heat-up rate starting from 450 µm at 4 K/s and reaching 100 µm at 8 K/s and more.

These experiments enable to propose different modes of clad failure at high temperatures depending on the heat-up rate:

- at high heat-up rates, the outer oxide scale which was formed in the pre-oxidation stage, is partially dissolved by molten Zircaloy during heating, and the thinned oxide layer is broken by hydrostatic pressure of molten Zircaloy;
- at low heat-up rates, the outer oxide scale which was formed in the pre-oxidation stage, continues to grow during heating, and the inner oxide layer appears on the pellet surface. Owing to the volumetric expansion of oxide, the gap volume unoccupied by the melt decreases and finally disappears, leading to a failure of the oxide scale due to incompressible molten Zircaloy pressure.

9   TESTS ON SIMULTANEOUS UO₂ AND ZRO₂ DISSOLUTION

For the simulation of fuel element dissolution process six scoping tests at 2100 °C on simultaneous UO_2 and ZrO_2 dissolution by molten Zircaloy were performed. The appearance of the post-test specimens is shown in Figure 8. The dissolution of ZrO_2 was very rapid. After ~ 225 s the rod in the melt had completely dissolved, so that the $Zr_{dissolved}/Zr_{total}$ ratio remained approximately constant at longer times.
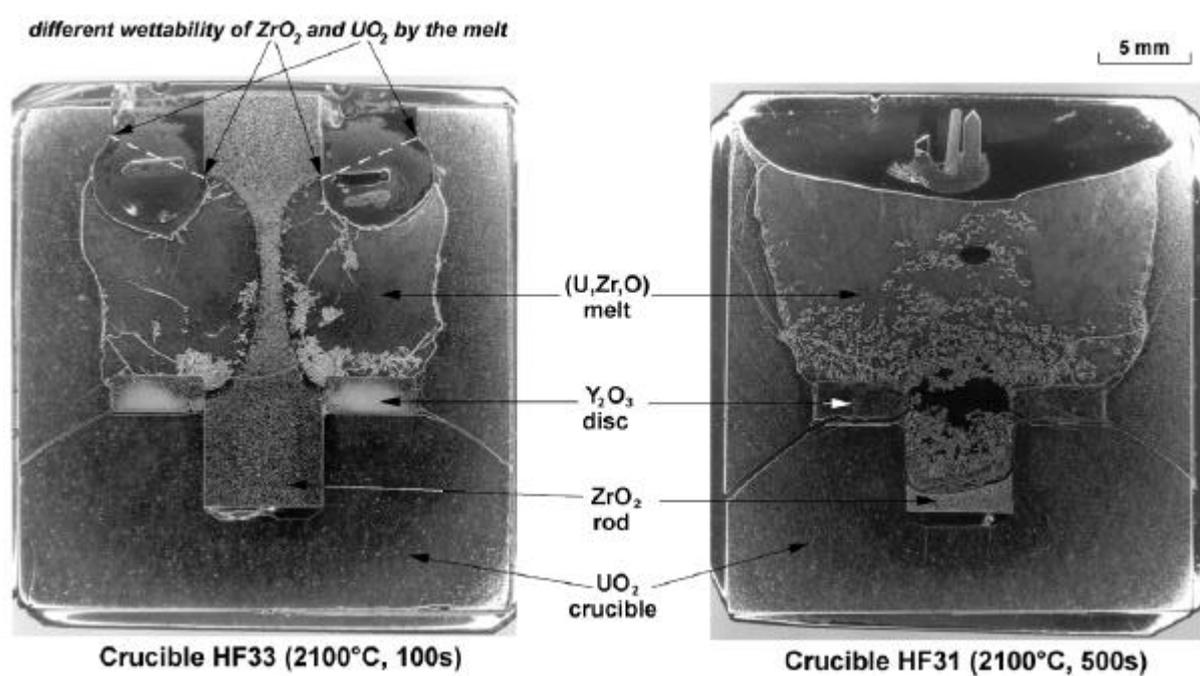

Figure 8. Simultaneous UO_2/ZrO_2 dissolution by molten Zircaloy

Results of the tests on simultaneous dissolution of UO_2 crucible and ZrO_2 rod were rather surprising, since the final U content in the melt in these tests was significantly higher (≈

63 wt.%) than in the previous tests without Ziconia rod at the same temperature 2100°C ($\approx$ 56 wt.%). On the other hand, the amount of ZrO_2 dissolved in these new tests ($Zr_{dissolved}/Zr_{total} \approx 0.25$) was also significantly higher in comparison with the previous ($Zr_{dissolved}/Zr_{total} \approx 0.1$) tests on single ZrO_2 dissolution. Therefore, one can conclude that the dissolution rates and amounts of both ceramic materials UO_2 and ZrO_2 were significantly higher in the tests with simultaneous dissolution of UO_2 and ZrO_2, in comparison with the tests where these materials were dissolved separately. This conclusion is very important from the point of view of the model application to the real accident conditions.

A comprehensive quantitative description of the simultaneous dissolution applicable to fuel rods can only be obtained on the basis of new tests. Additional studies are proposed on this topic in the COLOSS project of the EU 5th Framework Program at RIAR (Dimitrovgrad).

10   CONCLUSIONS

Regarding fuel rod liquefaction and related impact on clad failure, significant experimental results and models have been produced during the last 15 years. This effort enabled the extension of the corresponding database and the interpretation of the UO_2 and ZrO_2 liquefaction at temperatures significantly lower than the melting points of core ceramic components involved.

Two different physical-chemical phenomena determine the dissolution process:
-   mass transfer due to convection in the melt,
-   oxygen diffusion from the crucible matrix to the melt.

Apparent contradictions between previous databases on UO_2 and ZrO_2 dissolution could be explained in terms of crucible sizes, UO_2/Zr (or ZrO_2/Zr) mass ratios and melt surface to melt volume ratios (S/V). UO_2 dissolution and ZrO_2 dissolution models were proposed, able to reproduce the different experimental results obtained on UO_2 and ZrO_2 dissolution.

These results have a directly exploitable form for the implementation in plant analysis codes for modelling of separate ceramic dissolution. To reach the applicability stage of simultaneous dissolution modelling, additional research of UO_2 and ZrO_2 dissolution by molten Zry is needed.

REFERENCES

[1] P. Hofmann. "Current knowledge on core degradation phenomena, a review", *J. Nucl. Mater*. **270** (1999) 194-211.

[2] P. J. Hayward, P. Hofmann, J. Stuckert, A. Miassoedov, M. S. Veshchunov, A. V. Berdyshev. "UO_2 Dissolution by Molten Zircaloy. New Experimental Results and Modelling." FZKA 6379, Forschungszentrum Karlsruhe, Dezember 1999.

[3] M. S. Veshchunov and P. Hofmann, "Dissolution of Solid UO_2 by Molten Zircaloy", *J. Nucl. Mater*. **209** (1994) 27 – 40.

[4] B. Adroguer et al. "Corium Interactions and Thermochemistry". FISA 99 Symposium: EU Research in Reactor Safety. EUR-19532-EN, 2000

[5] P. Hofmann, J. Stuckert, A. Miassoedov, M. S. Veshchunov, A. V. Berdyshev, A. V. Boldyrev. "ZrO_2 Dissolution by Molten Zircaloy and Cladding Oxide Shell Failure. New Experimental Results and Modelling." FZKA 6383, Forschungszentrum Karlsruhe, Dezember 1999.